Molecular Crystals and Liquid Crystals
Publication details, including instructions for authors and subscription information:
http://www.tandfonline.com/loi/gmcl20

Defect-Related Photoconductivity and Mobility Effects in TlBr

V. Kažukauskas [a], A. Ziminskij [a], G. Davidyuk [b], V. Bozhko [b] & G. Mironchuk [b]

[a] Department of Semiconductor Physics and Institute of Applied Research of Vilnius University, Vilnius, Lithuania

[b] Volyn National University, Lutsk, Ukraine

Version of record first published: 28 May 2010

To cite this article: V. Kažukauskas, A. Ziminskij, G. Davidyuk, V. Bozhko & G. Mironchuk (2010): Defect-Related Photoconductivity and Mobility Effects in TlBr, Molecular Crystals and Liquid Crystals, 522:1, 82/[382]-88/[388]

To link to this article: http://dx.doi.org/10.1080/15421401003725081

Mol. Cryst. Liq. Cryst., Vol. 522: pp. 82/[382]–88/[388], 2010
Copyright © Taylor & Francis Group, LLC
ISSN: 1542-1406 print/1563-5287 online
DOI: 10.1080/15421401003725081

Defect-Related Photoconductivity and Mobility Effects in TlBr

V. KAŽUKAUSKAS,[1] A. ZIMINSKIJ,[1] G. DAVIDYUK,[2]
V. BOZHKO,[2] AND G. MIRONCHUK[2]

[1]Department of Semiconductor Physics and Institute of Applied
Research of Vilnius University, Vilnius, Lithuania
[2]Volyn National University, Lutsk, Ukraine

Photoelectrical and current transient properties of TlBr were investigated in the temperature region from −20°C up to +20°C, in which effect of the ionic conductivity changes significantly. Non-monotonous conductivity change with temperature was identified, demonstrating mobility-related maximum superimposed on a band-to-band generation conductivity growth. This maximum could be caused by the recharge of the scattering centre at about 1.65 eV. Presence of such centre was confirmed by the photocurrent spectra. From spectral dependencies defect-related transitions at 0.55; 0.83, 1.1; 1.32 and 1.65 eV were identified, being dependent on sample prehistory, i.e., its excitation by light and/or voltage. The transient photocurrent kinetics have demonstrated a complex behaviour that could be explained by the combined influence of electron generation/recombination processes superimposed upon the effect of ionic conductivity. The results indicate that ionic conductivity can take place also at −20°C, though its influence is less because of the thermally activated character.

Keywords Carrier transport; defects; electronic conductivity; ionic conductivity; TlBr

PACS 72.20.-i; 72.20.Jv; 72.40.+w; 72.80.Jc

I. Introduction

Thallium bromide (TlBr) is an attractive and promising material for X- and γ-ray spectroscopy because of its wide bandgap (2.68 eV), high density (7.56 g/cm^3) and high atomic numbers (Tl: 81 and Br: 35) [1–3]. Such collection of the attractive properties ensures a high photon stopping efficiency. The pixellated TlBr γ-rays detectors had demonstrated energy resolutions of 6.7 keV (5.5%) FWHM and 22.3 keV (3.4%) FWHM for 122 and 662 keV gamma-rays, respectively [2,3]. Nevertheless one of the main problems still hindering practical applications of TlBr is presence of the ionic conductivity, which sensitively depends on the temperature [4] and makes device characteristic unstable in time. It causes, e.g., degradation of

---

Address correspondence to V. Kažukauskas, Department of Semiconductor Physics and Institute of Applied Research, Vilnius University, Saulėtekio 9, bldg. 3, LT-10222 Vilnius, Lithuania. E-mail: vaidotas.kazukauskas@ff.vu.lt

spectroscopic performance because of the polarization phenomena if devices are operated at the room temperature [2].

II. Samples and Experiment

TlBr single crystals were grown by the Bridgman–Stockbarger method. The samples with dimensions of about $4 \times 3 \times 1\,\mathrm{mm}^3$ were provided with the evaporated gold contacts. They were investigated in the temperature region from −20°C up to +20°C, in which effect of the ionic conductivity changes significantly [4]. Experiments were carried out in a four-stage Peltier cooler cryostat. It enabled cooling down the samples by about 50°C from the reference temperature of the water supply. To enable optical excitation of the sample, an optical window was mounted into the cryostat. The current flowing through the sample was measured by a digital electrometric voltammeter Keithley 6517 A. To investigate the photoelectrical spectral dependencies optical excitation of the sample by monochromatic light from a Leitz monochromator was used. The monochromator was updated to ensure numerical control of the light wavelength and intensity. The temperature of the sample was controlled by a calibrated Si temperature sensor mounted into the cooler nearby the sample. Its resistivity was measured by a digital multimeter Fluke 45. All the data readout and experiment control were performed numerically from a PC via GPIB, RS-232 and LPT interfaces. In order to prevent the long-living sample polarization and its irreversible degradation, low applied electric fields of less than 150 V/cm were used. A number of experiments were carried out at the electric field strength over the sample as low as 3.8 V/cm (1.5 V). Nevertheless, because of the low signals and noise, series of measurements were repeated at 15, 30 and 60 V biases, giving the more informative results. The presented results were obtained at electric field strengths of about 150 V/cm.

III. Results and Discussion

III.1. *Temperature Dependencies of Current and Mobility*

To test the contact properties, the Current – Voltage (IV) curves were measured at different temperatures. The IV curves were symmetrical and linear in all cases, evidencing suitability of the used contacts. From these data we have evaluated sample resistance at 20°C being $R = 4.2 \times 10^{10}\,\Omega$ and its conductivity of about $(3\text{–}4) \times 10^{-10}\,\Omega^{-1}\,\mathrm{cm}^{-1}$. The temperature dependence of the sample conductivity is presented in Figure 1. It can be seen that in the temperature region of 258–278 K conductivity demonstrates a sharp maximum. It is superimposed on the conductivity growth due to the band-to-band generation having the activation energy of about $E_G/2$. This maximum could be mobility-related as it is evidenced in Figure 1. Similar conductivity behaviour was revealed by impedance spectroscopy in [5], though we haven't observed it in the samples with lower thermal activation energy of about 0.78 eV [6]. The height and position of the maximum were dependent on the sample prehistory (Fig. 2a). Nevertheless, the maximum, once reached, did not vanish with time (inset of Fig. 2b), though long current relaxations took place. Such relaxations might be due to either persistent conductivity in disordered materials [e.g., 7–9] or ionic conductivity of TlBr.

The thermal activation energy of this mobility-related maximum was up to $1.65 \pm 0.15\,\mathrm{eV}$ in different samples, evidencing that it was rather caused by the recharge of the scattering centre, and not by weakening ionized impurity scattering.

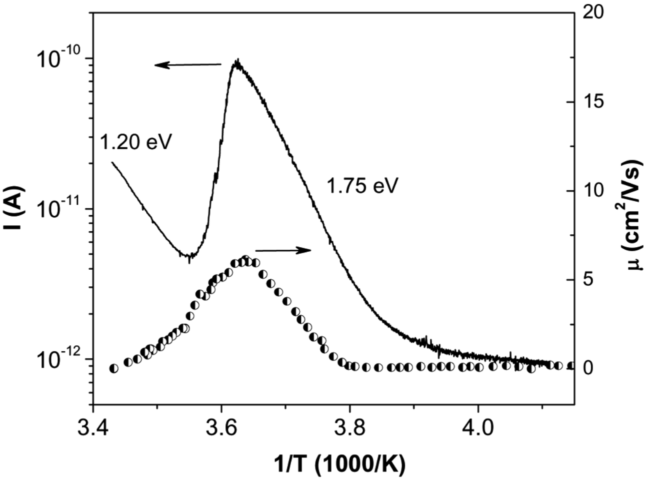

Figure 1. Temperature dependence of the sample current and Hall mobility.

III.2. *Defect Levels Identified by Photocurrent Spectroscopy*

To discriminate the defect level spectra we have investigated the photocurrent dependencies on the quantum energy of the exciting light as it is presented in Figure 3a. The spectra were analysed using Lucovsky photoionization model [10]:

$$I \sim n_M \Delta E_M^{0.5} (h\nu - \Delta E_M)^{1.5} / (h\nu)^3, \tag{1}$$

here E_M is optical activation energy of the deep trap, n_M is density of the trapped carriers, and $h\nu$ is quantum energy of the exciting light. A band-to-band generation starts at about 2.75 eV. Current drop that takes place at the higher energy side could be associated with the increasing absorption and, as a consequence, growing

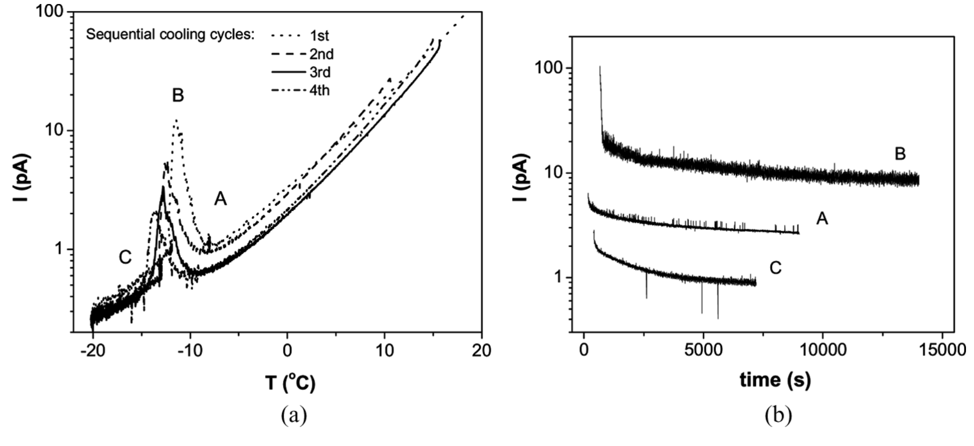

(a) (b)

Figure 2. (a) Change of the current maxima position and height during subsequent cooling cycles. Letters A-C mark characteristic temperatures at which dark current relaxations were measured as presented in (b).

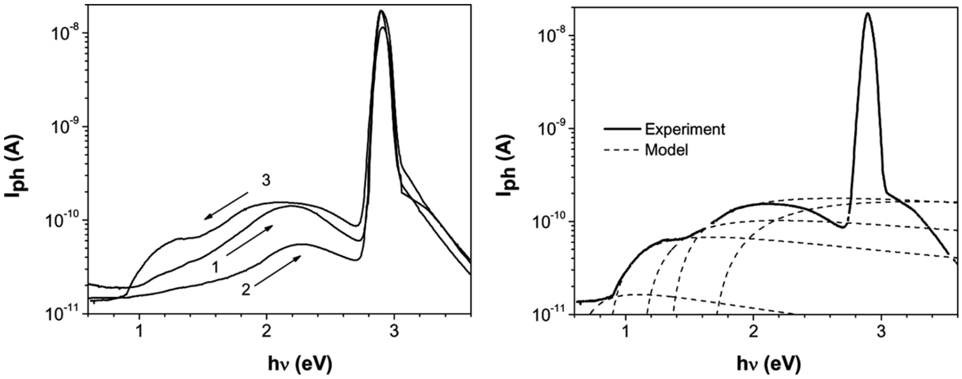

(a) (b)

Figure 3. (a) Photocurrent spectra at −20°C. Curve 1 was obtained after relaxation of the unbiased sample in the dark for 20 h. Curves 2 and 3 were measured after keeping the sample with 60 V bias at the room temperature for 6 hours, afterwards cooling it down and scanning spectra in different directions. Measurement directions are indicated by the arrows. (b) Fitting of the curve 3 by Eq. (1).

influence of the surface recombination. The most interesting results related to the defect bands appear at low temperature in the region between 1 eV and 2.5 eV. From the spectral dependencies of photocurrent several defect-related maxima in this region were identified, being dependent on the sample prehistory. Fitting of the experimental curves, the example of which is presented in Figure 3b revealed the following photoionization energies: 0.55; 0.83, 1.1; 1.32 and 1.65 eV. The last value coincides with that obtained from Figure 1, confirming presence of the defect level that can be neutralized, causing mobility growth. Characteristically, defect bands in the region between 1 eV and 2.5 eV were dependent on sample prehistory. All the curves in Figure 3a except 3 were measured starting from the low quantum energies. The measurement directions are indicated by the arrows. Curve 1 was obtained after relaxation of the sample in the dark for 20 hours without applied voltage. Meanwhile curves 2 and 3 were obtained after keeping the sample with applied 60 V voltage at the room temperature for 6 hours, afterwards cooling it down and scanning the spectra in different directions. The defect-related shoulders at about 0.83 and 1.1 eV used to appear if the spectra were scanned starting from the higher quantum energies. Meanwhile influence of the levels at 1.32 and 1.65 eV used to decrease if the sample was kept biased for several hours.

Similar complicated defect structure was also revealed by PL in [11]. The luminescence in the range 1.5–2.0 eV was observed under X-ray excitation and was attributed to several recombination centers [11], meanwhile absorption band at 1.1 eV was observed in the short-lived absorption spectra under pulsed electron beam excitation in [12] and it was explained to be due to hole trapped at cation vacancy ($Tl^{2+}Vc^{-}$). This centre can be created if hole is trapped by a pre-irradiation vacancy, as well as result from the radiation-induced Frenkel pair formation ($Tl^{2+}Vc^{-}$ and interstitial Tl_i^0). Our results indicate that such vacancy can also be light-induced, even though intensity of the light from monochromator is low. Therefore we have investigated the photocurrent transient effects.

III.3. *Diffusion Related Photocurrent Relaxations*

Kinetics of the photocurrent were measured at different temperatures upon the excitation of the sample by the light with the wavelength from the maximum absorption region. Figure 4a represents general and repeatable tendencies. Similar behaviour, though less expressed, was also observed without light excitation. The notable feature is presence of two different trends. When the light is turned on, after the sharp jump, current decrease starts, which is replaced by the growth until saturation. These thermally activated processes followed the exponential dependencies with the single time constants (Fig. 4b). Though the time constants of current decay and its growth were differing by about two orders of magnitude but their thermal activation energy values of about 0.24–0.27 eV were the same within the range of accuracy.

Therefore it can be supposed that the photocurrent kinetics is caused either by two different competitive processes or by a single complex process. In the first case the current decrease could be ascribed to the faster electronic process, i.e., trapping

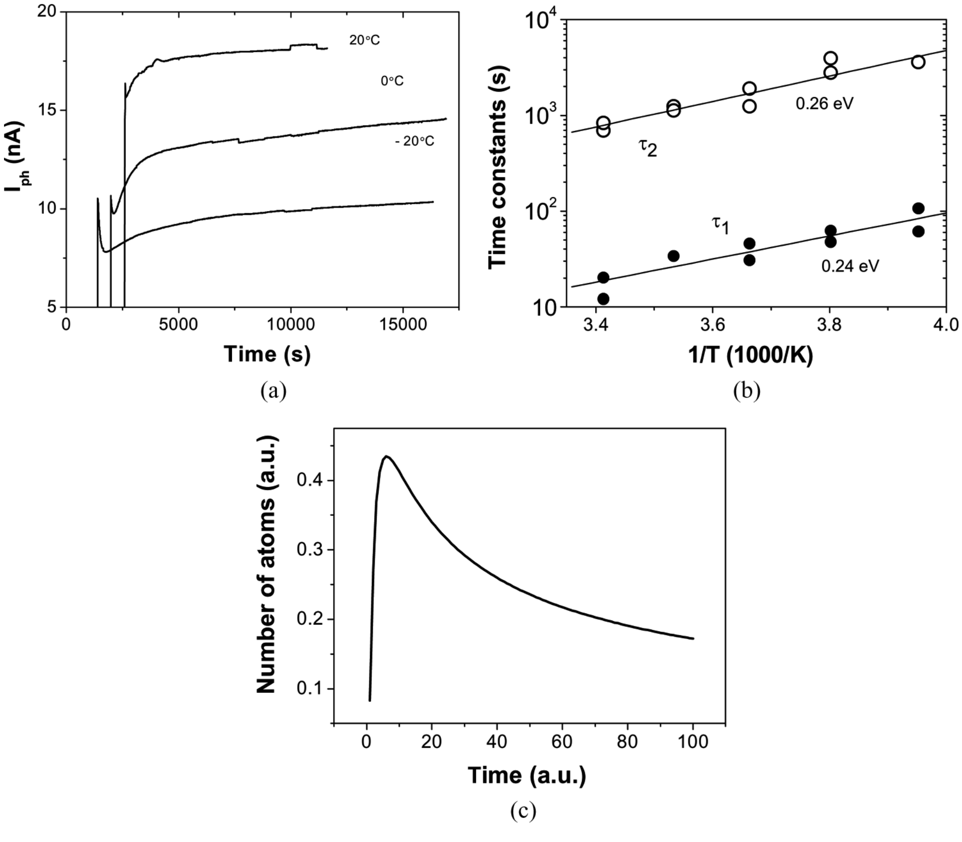

(a) (b)

(c)

Figure 4. (a) Current transients at different temperatures, after the onset of the light excitation corresponding to the photoconductivity maximum. Curves are shifted in time for the sake of convenience. (b) Dependence of the averaged time constants τ_1 and τ_2, describing current decrease and the following growth, respectively. (c) Model curve, representing number of extraneous atoms diffusing from a limited source at a certain space point depending on time – Eq. (2).

and/or recombination of light-generated carriers to the defect centres. This process could be similar to the known mechanism of the thermal quenching. The following current increase might be attributed to the growing ionic conductivity of Tl^+ ions, as observed in [5].

Nevertheless the similar thermal activation energies of both time constants point out that they might be attributed to the single process. Similar non-monotonous behaviour is characteristic for the diffusion from a limited material source [13]. In such case the total number of extraneous atoms at a certain point is given by:

$$N = \frac{A}{\sqrt{t}} \exp\left(-\frac{B}{t}\right), \tag{2}$$

here A and B are diffusion- and material-related constants, and t is time.

A model curve calculated according to Eq. (2) is presented in Figure 4c. It can be seen that this curve qualitatively demonstrates inverse dependence in time as compared to the experimental traces. Therefore, if one assumes that transport properties are given by carrier and/or ion mobility that are limited by a varying number of scattering centres, then at least qualitative coincidence could be obtained, if mobility μ is supposed to demonstrate the inverse proportionality to the number N of scattering centres:

$$\mu \sim 1/N. \tag{3}$$

Similar kinetic effects, just less expressed, were also observed without light excitation. The signal was much smaller, and consequently, in many cases distorted by the already mentioned noise effects, especially at low temperatures. Therefore we could not make any definite quantitative evaluations. At 20°C temperature the already described current growth was observed after switching on the bias. Nevertheless at lower temperatures only current decrease took place without any indications of its further growth, at least within the experiment duration of up to 2×10^4 s. This is in contrast to the described behaviour observed with light excitation. The characteristic time constants were much longer as well. Notably that the very fast initial current drop with no kinetics and residual effects took place at the moments when the bias was switched off.

Summary and Conclusions

We had investigated photoelectrical and current transient properties of TlBr in the temperature region from −20°C up to +20°C, in which effect of the ionic conductivity is pronounced. Sample conductivities at 20°C were about $(3\text{–}4) \times 10^{-10}\,\Omega^{-1}\,\text{cm}^{-1}$.

Current peculiarities were revealed that could stand for both electronic and ionic conductivities. Non-monotonous conductivity variation with temperature was identified, demonstrating mobility-related maximum that was superimposed on an intrinsic conductivity growth. This maximum could be caused by the recharge of the scattering centre at about 1.65 eV. Presence of such centre was confirmed by the photocurrent spectra.

From the spectral dependencies several defect-related transitions at 0.55; 0.83, 1.1; 1.32 and 1.65 eV were identified, being dependent on sample prehistory, i.e., its excitation by light and/or voltage. The defect-related shoulders at about 0.83

and 1.1 eV used to intensify if the spectra were scanned from the higher quantum energies. Meanwhile influence of the levels at 1.32 and 1.65 eV used to decrease if the sample was kept biased for several hours.

The photocurrent kinetics had demonstrated a complex structure in which its decrease was changed by the growth. The thermal activation energy of the time constants of both processes was found to be 0.24–0.27 eV. Such complex behaviour could be explained either by the combined trapping and/or recombination of light-generated carriers to the defect centres, followed by the growing ionic conduction or by the variation in time of the ion diffusion-related scattering. Our results, in contrast to [4], demonstrate that ionic conductivity can take place also at −20°C, though its influence is less because of the thermally activated nature. Moreover, even low intensity intrinsic light excitation might be effective in capacitating ionic conductivity.

Acknowledgments

This work was supported by the Lithuanian and Ukrainian Ministries of Education and Science and Lithuanian State Studies and Science Foundation (project No. V-18/2009). The samples were kindly provided by Brucker Baltic (dr. V. Gostilo and dr. M. Shorohov).

References

[1] Sellin, P. J. (2003). *Nucl. Instrum. Meth. A*, *513*(1–2), 332–339.
[2] Hitomi, K., Matsumoto, M., Muroi, O., Shoji, T., & Hirarate, Y. (2002). *IEEE Trans. Nucl. Sci.*, *49*(5), 2526–2529.
[3] Hitomi, K., Matsumoto, M., Muroi, O., Shoji, T., & Hirarate, Y. (2001). *J. Cryst. Growth*, *225*(2–4), 129–133.
[4] Onodera, T., Hitomi, K., & Shoji, T. (2006). *Nucl. Instrum. Meth. A*, *568*(1), 433–436.
[5] Vaitkus, J., Banys, J., Gostilo, V., Zatoloka, S., Mekys, A., Storasta, J., & Žindulis, A. (2005). *Nucl. Instrum. Meth. A*, *546*, 188–191.
[6] Kažukauskas, V., & Jurgilaitis, A. (2008). *Mol. Cryst. Liq. Cryst.*, *485*, 825–834.
[7] Shklowskii, B. I., & Efros, A. L. (1971). *Zh. Eksp. Teor. Fiz.*, *61*, 816 (in Russian).
[8] Shklowskii, B. I., & Efros, A. L. (1979). *Electronic Properties of Doped Semiconductors*, Nauka: Moscow, (in Russian).
[9] Sheinkman, M. K., & Shik, A. J. (1976). *Phys. Tekh. Polupr.*, *10*(2), 209–223 (in Russian).
[10] Lucovsky, G. (1965). *Solid State Comm.*, *3*, 299–302.
[11] Grigorjeva, L., & Millers, D. (2002). *Nucl. Instrum. Meth. B*, *191*, 131–134.
[12] Grigorjeva, L., & Millers, D. (1998). *Electrochemical Soc. Proc.*, *25*, 438–443.
[13] Pavlov, P. V., & Khohlov, A. V. (1985). *Solid State Physics*, High School: Moscow (in Russian).